AgriEngineering

Article

Design, Fabrication, and Performance Evaluation of a Food Solar Dryer

Md. Suman Rana [1], A. N. M. Arifur Rahman [2], Rakib Ahmed [1], Md. Pallob Hossain [1], Md. Salim Shadman [1], Pranta Kumar Majumdar [1], Kh. Shafiqul Islam [2] and Jonathan Colton [3,*]

[1] Department of Agro Product Processing Technology, Jashore University of Science and Technology, Jashore 7408, Bangladesh; sumanrana@just.edu.bd (M.S.R.)
[2] International Maize and Wheat Improvement Centre (CIMMYT), Dhaka 1212, Bangladesh
[3] George W. Woodruff School of Mechanical Engineering, Georgia Institute of Technology, Atlanta, GA 30332, USA
* Correspondence: jcolton@gatech.edu

Abstract: One of the oldest techniques for preserving food is drying. Dehydrating foods reduces their moisture content and increases their shelf life by preventing microbiological activity. Food placed on the ground to dry in the sun is a common sight in rural areas of low- and middle-income countries but requires a large amount of land and can lead to food degradation by overexposure to the sun, insects, and vermin. This study designed, fabricated, and evaluated the performance of a solar dryer in comparison to direct sun drying for efficiency and product quality, utilizing bananas and potatoes as representative foods. The dryer was produced and tested within the context of Bangladesh, unlike other commercial devices. With its mild steel frame, fan, solar collector, and DC battery, the dryer achieved a drying efficiency of 49.2% by reaching a drying chamber temperature of 71 °C, which is 30 °C higher than ambient. Drying times were decreased, and samples of potatoes and bananas reached equilibrium moisture content in 6 h as opposed to 9 h for direct sun drying. The moisture content of solar-dried foods was between 12 and 13 percent, making them appropriate for long-term storage. Bioactive substances such as phenolic content and DPPH scavenging activity were reduced by 18% and 21%, respectively, in comparison to direct sun drying. Quality assessments showed that there was little loss in color and nutrients for solar-dried samples. With a one-year payback period, an economic attribute of 3.26, and a life cycle benefit of BDT 310,651 (USD 2597.68), economics show the dryer's feasibility. The solar dryer functioned faster than direct sun drying due to its significantly higher heat generation. The solar dryer was more efficient, effective, and economic within the context of Bangladesh and other low- and middle-income countries.

Keywords: design; food preservation; food quality; post-harvest loss; solar drying

Citation: Rana, M.S.; Rahman, A.N.M.A.; Ahmed, R.; Hossain, M.P.; Shadman, M.S.; Majumdar, P.K.; Islam, K.S.; Colton, J. Design, Fabrication, and Performance Evaluation of a Food Solar Dryer. *AgriEngineering* **2024**, *6*, 4506–4523. https://doi.org/10.3390/agriengineering6040257

Academic Editor: Marcello Biocca

Received: 3 October 2024
Revised: 22 November 2024
Accepted: 25 November 2024
Published: 28 November 2024

1. Introduction

One of the oldest techniques for preserving food is drying. Dehydrating foods reduces their moisture content and increases their shelf life by preventing microbiological activity [1]. Improving the quality and quantity of food products and reducing post-harvest losses are ongoing challenges for agricultural producers. In fact, these cannot be accomplished without expensive and complex techniques and equipment, which raise costs and energy usage [2]. One of the primary phases of post-harvest processing is storage, where significant degradation may occur [3]. Food placed on the ground to dry in the sun is a common sight in rural areas of low- and middle-income countries. But there are many drawbacks to this practice. It needs a large surface area and prolonged exposure to sunshine, and it is dependent on the climate. The dried product may deteriorate as a result. Moreover, drying large quantities of food is not possible with this method [4]. As a sustainable and eco-friendly option, solar dryers are essential for increasing food security and reducing post-harvest losses in agricultural environments. The sun provides more than

99.99% of the world's energy [5]. By harnessing the power of the sun year-round [6], solar dryers offer an effective means to remove moisture from a diverse array of agricultural commodities, ranging from fruits and vegetables to cereals and herbs, while eliminating the need for electricity and fossil fuels [7]. This reliance on solar radiation underscores the importance of the thoughtful design and fabrication of solar dryers. Indeed, a successful design must carefully account for factors such as the specific type and volume of foods slated for drying, prevailing sunlight intensity and duration, local climate conditions, and cost-effectiveness [8]. In navigating this design landscape, many options exist, from straightforward passive systems to sophisticated active setups containing fans and temperature control mechanisms. However, regardless of design complexity, the overarching goal remains consistent: to optimize moisture removal, solar energy absorption, and airflow while minimizing heat loss and cost [7]. Heat is required during the drying process to remove moisture from the material, and air movement aids in removing the evaporated moisture. The drying process involves two fundamental mechanisms [9]: the diffusion of moisture from inside a material to its surface and the evaporation of moisture from the surface into the surrounding air. The drying process involves mass and heat transfer and is affected by factors such as air velocity, humidity, and temperature. Once a design is completed, performance evaluation is required to determine its efficiency and efficacy. Critical parameters, including drying rate, moisture content reduction, and resultant product quality, must be measured and analyzed [10]. Beyond technical specifications, factors such as reliability, durability, and ease of operation affect a design's real-world utility, particularly in the eyes of farmers and food processors.

As the global community increasingly seeks energy-efficient and ecologically sound methods for food preservation, the importance of solar dryers continues to increase because they are beacons of hope for a more sustainable future. Consequently, sustained research efforts into the design and performance evaluation of solar dryers are indispensable, ensuring their continued evolution and widespread adoption in the quest for a more resilient and environmentally conscious food system [11]. Marinoni et al. [12] performed a similar study to the present one. They fabricated and tested a solar dryer suitable for use in developing countries. Their device was fabricated and tested in Europe rather than in developing countries. It used polycarbonate instead of glass for its transparent walls. Glass is more available and cheaper in most low- and middle-income countries. They focused almost exclusively on the color of the dried foods as their metric of quality, and their results are consistent with those in the present study.

In this study, the design of domestic solar dryers was improved by including a PE sheet sandwiched between two metal sheets to reduce heat loss from the outer surface of the dryer and fabricating it from thin sheets of stainless steel to reduce the initial cost of manufacture. The dryer was designed considering the limitations of manufacturers and operators in Bangladesh, which other commercial devices do not. Moreover, it ensured a quicker drying rate as compared to sun drying, thereby ensuring the retention of essential nutrients and reducing the chance of spoilage due to slow moisture diffusion and unhygienic conditions due to dust, insects, and rodents. In this paper, the performance of this improved solar dryer design within the manufacturing and operating contexts of Bangladesh and LMICs is evaluated, and the physicochemical properties of dehydrated products produced by this design are assessed.

2. Materials and Methods

2.1. Description of the Dryer

A photograph of the solar dryer is shown in Figure 1. Schematic diagrams and component details of the solar dryer are presented in Figure 2 and Table 1. The dryer utilizes forced convection and comprises a drying chamber, solar collector unit, blower fan, heating chamber, direct current (DC) battery, and switch control unit. The top of the drying chamber is covered with glass (4 mm) to transmit sunlight into the dying chamber. The drying chamber houses six drying trays arranged side by side in two columns, which are constructed from perforated stainless steel for efficient hot air circulation and ease of cleaning. These drying plates are supported on a mild steel frame fixed to the inner sidewalls of the drying chamber, allowing for their easy removal to load or unload the food products through the door, which is double partitioned. The trays are spaced 13 mm apart from each other to ensure uniform air circulation beneath and around the drying material. A chimney, also made from mild steel, is positioned at the top right corner of the drying chamber to expel the humid air from inside the chamber. The heating chamber frames are constructed from mild steel. The blower housing, which contains the axial fan and control switch, is mounted externally to the top right corner of the heating chamber. The fan draws in ambient air, which passes through the air inlet zone, where it is heated as it passes over the hot, mild steel surface and then flows through the drying chamber. A thermometer and a fan speed regulator measure the temperature of the drying chamber and control the fan speed. This allows for precise control of the drying process. The walls of the dryer, along with the air inlet zone, are constructed with double-layer mild steel sheets of 1 mm thickness. A 5 mm thick layer of polyethylene foam insulation is inserted between the metal sheets to reduce heat loss. The solar collector chamber is painted black to ensure effective absorption of solar radiation. Additionally, a solar panel is mounted onto a movable stand on the side of the dryer. The solar panel is connected to the battery via a solar charge controller, which in turn controls the fan to provide forced convection. The battery allows the fan to operate when the sun is not out, for example, when it is cloudy or during nighttime, helping to control the atmosphere inside the dryer. These additions represent improvements over other solar dryers available in Bangladesh.

Figure 1. Solar dryer.

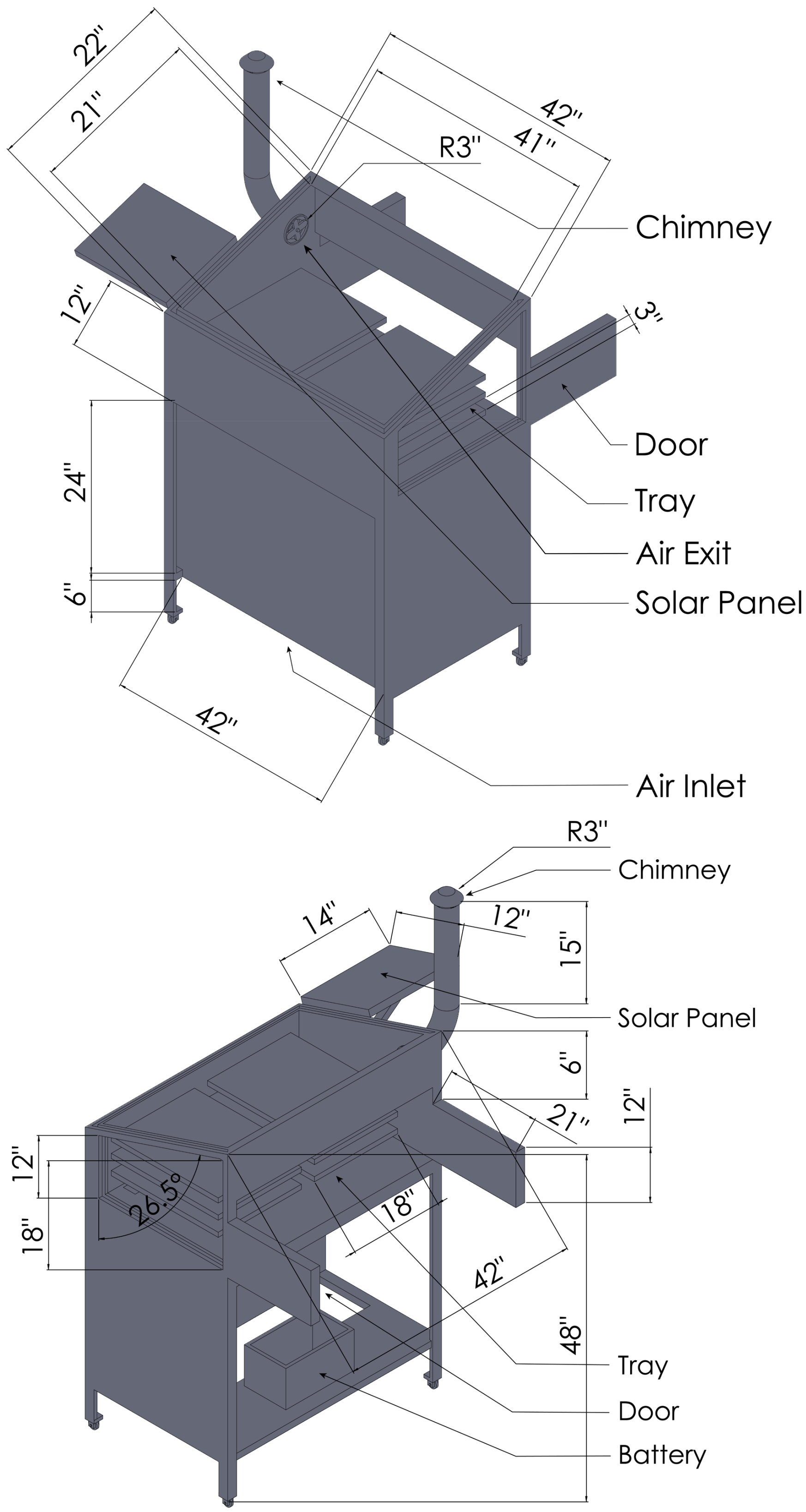

Figure 2. Solar dryer front and back views.

Table 1. Description of the solar dryer components and specifications.

Component	Specifications
Air inlet chamber	1016 mm × 610 mm
Air inlet port (2 ports) diameter	11.5 mm
Solar panel (monocrystalline solar panel)	356 mm × 305 mm
Fan housing	76 mm diameter
Drying chamber (trapezium shape)	1067 mm × 508 mm × (305 mm and 457 mm)
Door	533 × 305 mm inch (double door)
Tray	457 × 457 mm
Chimney coverer	76 mm diameter
Solar panel capacity	10 Watts
DC battery	12 Volts
Insulation (PE foam sheet)	5 mm
Display	Thermometer, power switch, regulator
Glass top	4 mm thick

2.2. Drying

Experiments were conducted in the Jashore Sadar, Jashore, Bangladesh in April 2024. The solar dryer was placed in an open space free from the shadows of trees and plants. The days were hot and sunny. The ambient temperature range was 36–42 °C with a relative humidity of approximately 66%. According to weather reports, the air velocity was 4.8 km/h. Drying took place between 9:30 a.m. and 4:30 p.m. The drying chamber temperature was evaluated at various fan speeds. The highest temperature recorded (71 °C) was when the exit air speed was the lowest and diminished with an increase in fan speed. The fan speed was optimized so that the exit air velocity was approximately 2 m/s for the best removal of moist air, which agrees with industrial process speeds of 2–3 m/s. The dryer was kept at the optimum fan speed for 10 days to investigate the temperature inside the drying chamber. The maximum and minimum temperatures of the dryer and ambient environment were recorded.

Bananas and potatoes were selected as experimental samples. Figure 3 shows the drying processes. First, the potatoes were sliced to 0.5 cm thickness. After that, they were blanched in boiling water for 2 to 3 min and arranged on a tray. The bananas were cut into quarters along their lengths and placed on the tray without blanching. One kilogram of each was placed in the dryer and allowed to dry. The temperatures of the drying chamber, collector, and ambient air were measured at 1 h intervals. The reductions in the weights of the samples were recorded periodically. Both types of food also were dried in direct sunlight without the aid of the solar dryer from 9:30 a.m. to 4:30 p.m. for comparison with the solar-dried products. When solar dryer samples achieved constant weight, they were removed from the dryer and kept in airtight containers for further analysis.

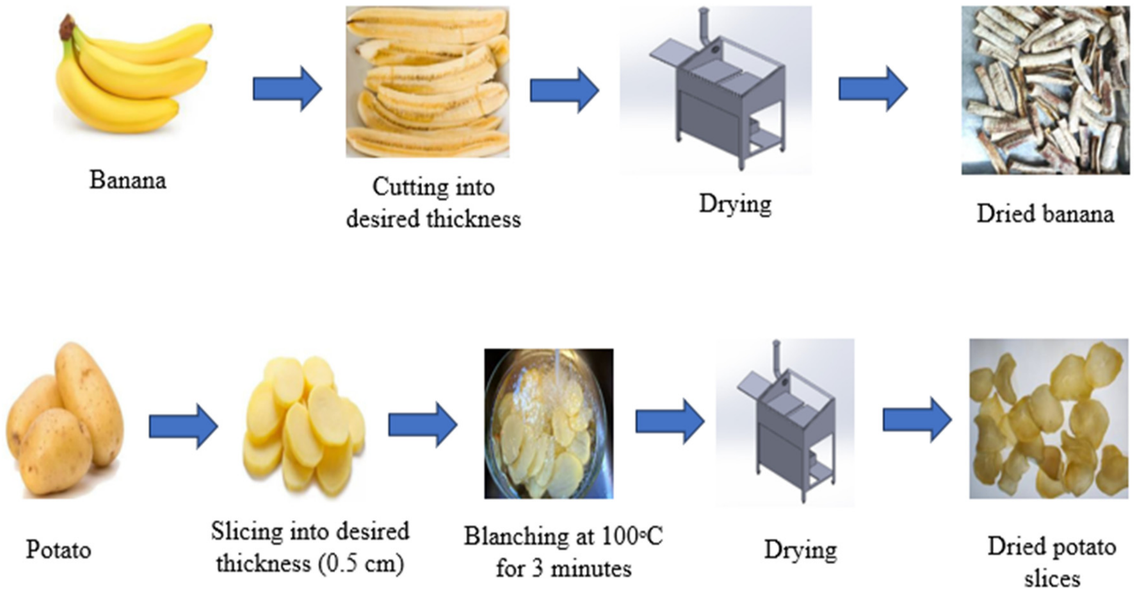

Figure 3. Flow chart of drying process of potato and banana.

2.3. Drying Performance Evaluation Equations

The general form of the energy equation applicable for a steady flow system can be expressed as Equation (1) [13]:

$$E_x = mC\left[(T - T_a) - T_a \ln\left(\frac{T}{T_a}\right)\right] \quad (1)$$

where E_x = energy (W), m = mass flow rate of air (kg/s), C = specific heat of air (kJ/kg-K), T = temperature of drying chamber (°C), and T_a = ambient temperature (°C).

Equation (2) describes the energy flow into the drying chamber:

$$E_i = mC\left[(T_i - T_a) - T_a \ln\left(\frac{T_i}{T_a}\right)\right] \quad (2)$$

where E_i = energy of inflow of drying chamber (W), and T_i = inlet air temperature (°C).

Equation (3) describes the energy flow from the drying chamber:

$$E_o = mC\left[(T_o - T_a) - T_a \ln\left(\frac{T_o}{T_a}\right)\right] \quad (3)$$

where E_o = energy of outflow of drying chamber (W), and T_o = temperature of outflow of drying chamber (°C).

However, during the solar drying process, the exergy losses are determined using Equation (4):

$$E_{loss} = E_i - E_o \quad (4)$$

Energy efficiency can be defined as the ratio of energy use in the drying of the product to the exergy of the drying air supplied to the system. Thus, the general form of energy efficiency is written as Equations (5)–(7) [13,14]:

$$\eta = \frac{E_o}{E_i} = 1 - \frac{E_{loss}}{E_i} \quad (5)$$

The moisture content (MC) of the sample is calculated as

$$MC_w = \frac{M_i - M_f}{M_i} \times 100 \quad (6)$$

$$MC_d = \frac{M_i - M_f}{M_s} \times 100 \tag{7}$$

where MC_w = moisture content in wet basis, MC_d = moisture content in dry basis, m_i = initial mass of sample, m_f = final mass of the sample, and m_s = mass of solids.

The drying rate (DR) is calculated as per Equation (8):

$$DR = \frac{M_w}{t} \tag{8}$$

where M_w = mass of water removed and t = time.

2.4. Drying Kinetics Equations

A thin layer drying model is used to evaluate the data obtained during drying at regular intervals. Fick's second law of diffusion describes mass transfer during drying, as shown in Equation (9):

$$\frac{\delta M}{\delta t} = \Delta^2 D_e M \tag{9}$$

where M = moisture content (dry basis), t = time, and D_e = effective diffusion coefficient.

When determining a solution for the unsteady state diffusion equation (Equation (9)) for one-dimensional transport for the case of initial uniform moisture distribution in the sample and negligible external resistance, approximate boundary conditions are expected. The solution for the moisture ratio (MR) of an infinite slab (with half thickness, l) when dried from one major face [15] is given by Equation (10):

$$MR = \frac{M_t - M_e}{M_o - M_e} = \frac{8}{\pi^2}\sum_{n=0}^{\infty}\frac{1}{(2n+1)^2}\exp\left[\frac{-(2n+1)^2\pi^2 D_e t}{l^2}\right] \tag{10}$$

For low values of M_e and moisture ratio < 0.6, Equation (6) reduces to Equation (11):

$$\frac{M_t}{M_o} = \frac{8}{\pi^2}\exp\left(\frac{-\pi^2 D_e t}{l^2}\right) = \frac{8}{\pi^2}\exp(-kt) \tag{11}$$

where $k = \frac{\pi^2 D_e}{l^2}$ = drying rate constants (sec^{-1}).

Rearranging Equation (11) gives Equation (12):

$$\ln\left(\frac{M_t}{M_o}\right) = \ln\frac{8}{\pi^2} - kt \tag{12}$$

A straight line results when ln(MR) is plotted against time (t). D_e, the effective diffusion coefficient, is determined by calculating the slope of the regression line, which is the drying rate constant, k. The Root Mean Square Error (RMSE) was calculated to assess the model's goodness of fit (based on the moisture ratio). Equation (13) [16] indicates that the model with the lowest RMSE values had the best goodness of fit.

$$RMSE = \sqrt{\frac{\sum(MR_{pr} - MR_{ex})^2}{N}} \tag{13}$$

2.5. Physicochemical Properties

2.5.1. Proximate Composition Analysis

Proximate composition such as moisture, protein, fat, and ash were measured as per the AOAC (Association of Official Analytical Chemists) method [17]. Total carbohydrates were measured using the subtraction method, as described by Pearson [18].

2.5.2. Color Analysis

Using a colorimeter (Chroma Meter CR400, Konica Minolta, Tokyo, Japan) and the L*, a*, and b* system, where L* stands for lightness, a* for redness (+)/greenness (−), and b* for yellowness (+)/blueness (−), the color degradation of potato and banana samples after drying was examined.

2.5.3. Bioactive Compounds

The method outlined by Majumder et al. [19] was used to determine the total phenolic content (TPC) of the potato and banana samples. A standard curve made with a gallic acid standard solution ranging from 0 to 100 milligrams per liter and represented as milligrams of gallic acid equivalent (GAE) per 100 g of sample was used to determine the TPC. Four milliliters of 7.5% Na_2CO_3 at a concentration of one milligram per milliliter was added to each sample, along with a 1:10 volume-by-volume Folin–Ciocalteu reagent. Color was obtained by vortexing the liquid for 15 s and then heating to 40 °C for 30 min. The absorbance was measured at a wavelength of 765 nm. Gallic acid served as the standard, and a calibration curve was created using acetone water (80:20 v/v) containing gallic acid at concentrations ranging from 0 to 13 mg/mL.

With a few minor adjustments, the procedure outlined by Chhetry et al. [20] was used to calculate the total flavonoid content. The ethanolic extract was first made at a concentration of 1 mg/mL. The extract then was diluted with 0.3 mL of a 5% $NaNO_2$ solution and 4 mL of purified water. After incubating for 5 min, 0.3 mL of a 10% $AlCl_3$ reagent solution was added, and the mixture was incubated for an additional 5 min. The mixture then was mixed with 2 mL of a 1 M NaOH solution. Additionally, a control solution without any samples was produced. To guarantee complete reactions, the reaction mixtures were allowed to incubate for 30 min at room temperature. Following incubation, a double-beam Scientific UV–Vis Spectrophotometer quantified absorbance at 430 nm. A standard calibration curve for quercetin was used to calculate the total flavonoid concentration.

A technique by Aboshora et al. [21] assessed the DPPH (2,2-diphenyl-1-picrylhydrazyl) free radical scavenging activity of dehydrated potato and banana samples. A 200 µL extract sample and 1.0 mL of 0.1 mM DPPH in methanol were combined as part of the process. The mixture was shaken and left to react for 20 min at room temperature. The absorbance at 517 nm was compared to methanol blanks to calculate the residual quantity of DPPH free radical. Equation (14) was used to compare the absorbance drop to the control in order to determine the percentage scavenging effect.

$$\text{Scavenger activity } \% = \frac{\text{Absobance(control)} - \text{Asorbance(sample)}}{\text{Absorance(control)}} \times 100 \tag{14}$$

2.5.4. Sensory Analysis

Using the approach of Kumar et al. [22], an organoleptic evaluation was conducted to determine the goods' color, texture, taste, scent, and general acceptability. Before being evaluated, every sample was kept in an ambient environment. A panel consisting of 15 judges assessed the samples' color, taste, scent, texture, and general acceptability using a cell distribution on a 9-point Hedonic scale. Students from Jashore University of Science and Technology were chosen to serve as the judges. They were between the ages of 18 and 22. Seven of the judges were men and eight were women.

2.6. Cost Analysis

An economic analysis of the solar dryer was conducted by determining the dryer's life cycle cost (LCC) and life cycle benefit (LCB). Additionally, to assess the dryer technology's economic feasibility, the economic attributes and payback period (PBP) were calculated. Table 2 shows the initial cost of the solar dryer.

Table 2. Initial cost of the solar dryer.

Item with Specification	Cost (BDT)	Cost (USD)
Fan (12 V)	350	2.93
Solar Pannel (10 W)	650	5.44
DC Battery (12 V)	12,500	10.03
Insulator (PE foam sheet)	350	3.93
Aluminum net	370	3.09
Paint and accessories	930	7.78
MS sheet	6310	52.76
MS angle bar	6090	50.92
Glass (4mm)	1530	12.79
Thermometer	150	1.25
Pipe	275	2.30
Total Cost	29,505	246.72

2.6.1. Life Cycle Cost (LCC)

The present value of all the expenses associated with the sun drying system over its lifetime, adjusted for the time value of money, is the direct solar dryer's life cycle cost (LCC). The techniques of Barnwal andTiwari [23] and Singh et al. [24] were used to estimate the LCC (Equations (15) and (16)). According to Table 2, the initial investment (Pi) is BDT 29,505 (USD 246.72). The annual cost of operation and maintenance (O&M) including labor is BDT 9000 (USD 75.26). The dryer's life was estimated to be ten years, and the salvage value was calculated at ten percent of the initial investment.

$$\begin{aligned}\text{LLC} = \text{initial cost of unit } (\text{P}_\text{i}) + \text{operational and maintenance expense including labor cost } (\text{P}_\text{w}) \\ -\text{present worth of salvage value } (\text{P}_\text{s})\end{aligned} \quad (15)$$

$$\text{LCC} = \text{P}_\text{i} + \text{P}_\text{w} \times \frac{\text{X}(1 - \text{x}^\text{n})}{(1 - \text{X})} - \text{SV}(1 - \text{i})^{-\text{n}} \quad (16)$$

where n = life of the dryer (10 years), e = annual escalation in cost (4%), I = interest or discount rate (10%), and $\text{X} = \frac{1+\text{e}}{1+\text{i}}$ = 0.945.

2.6.2. Life Cycle Benefits (LCBs)

The annual benefit was obtained by adopting a thorough drying cycle for the product using the methods followed by Barnwal and Tiwari [23] and Singh et al. [24]. Three trials were carried out while drying potatoes and bananas. The potato quantity in each trial was 6 kg, which cost around BDT 240 (USD 2.00). The dried potato weighed roughly 1 kg. Potato powder costs approximately BDT 350 (USD 2.93) on average, according to both online and offline markets. Therefore, BDT 110 (USD 0.92) per day can be earned each day. Similarly, 8 kg of bananas (including peel) were purchased for BDT 200 (USD 1.67). After drying, about 1 kg of dried banana slices was obtained. The local market average price of sliced banana is approximately BDT 400 (USD 3.44). Therefore, about BDT 200 (USD 1.67) can be earned per day. If one considers that nine months have adequate sunlight to dry fruits and vegetables during the daytime, one excludes three months for extreme winter and rainy seasons. Then, the total annual benefit may be calculated as BDT 29,700 (USD 246.72) for potato and BDT 54,000 (USD 451.54) for banana. For calculating the life cycle benefit (LCB), the average annual benefit of potato and banana is considered.

Finally, the life cycle benefit may be calculated using Equation (17).

$$\text{LCB} = \text{R} \times \frac{\text{X}(1 - \text{X}^\text{n})}{1 - \text{X}} \quad (17)$$

where R is the annual benefit = BDT 41,850 (USD 349.94).

2.6.3. Economic Attribute

Economic attribute is the ratio of discounted benefits to the discounted values of all costs. Economic attributes were calculated according to Poonia et al. [25] using Equation (18).

$$\text{Economic Attributes} = \frac{\text{LCB}}{\text{LCC}} \quad (18)$$

2.6.4. Payback Period

The duration between cumulative net cash outflows and yearly net cash inflow is indicated by the payback period. According to Singh et al. [24], the payback period is computed using either LCC = LCB or LCC − LCB = 0. Therefore,

$$29505 + 9000 \times \frac{0.945(1 - 0.945^{n})}{1 - 0.945} = 41850 \times \frac{0.945(1 - 0.945^{n})}{1 - 0.945} \quad (19)$$

Solving for n yields n = 0.949 ≈ 1.

2.6.5. Statistical Analysis

Microsoft Excel (version 2019) was used to analyze the data. Statistical techniques used in the analysis included Analysis of Variance (ANOVA) and descriptive statistics, all performed at a 5% level of significance. The Least Significant Difference (LSD) test was used to compare means among groups. The data's central tendency and variability were summarized by presenting the results as mean ± standard deviation.

3. Results and Discussion

3.1. Drying Performance Evaluation

Figure 4 displays the evaluation of the drying chamber's internal temperature in relation to the outside temperature. After ten days of observation, the solar dryer's drying chamber reached its highest and lowest temperatures in the range of 66–69 °C and 45–48 °C, respectively, while the ambient temperature ranged between 39 and 43 °C and 35 and 38 °C. The evaluation revealed that the dryer's internal temperature generation was 30 °C higher than the outside temperature. This observation is similar to that of Kilanko et al. [26].

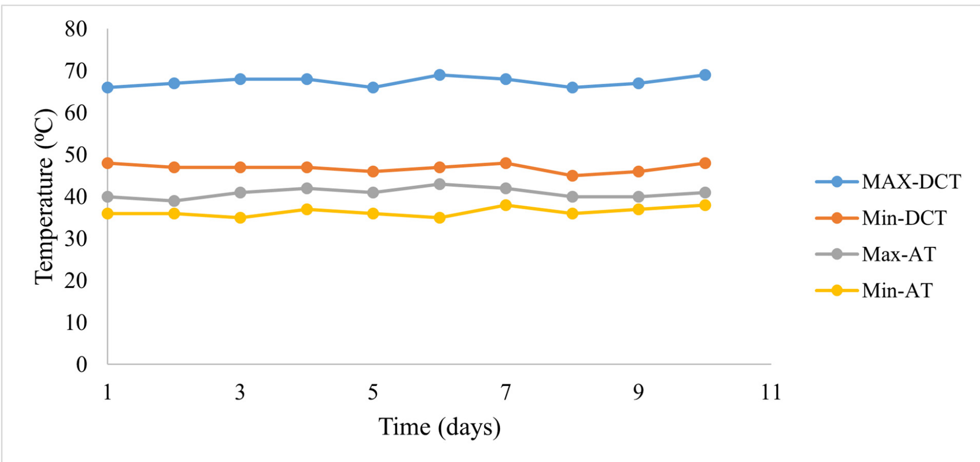

Figure 4. Dryer chamber and ambient temperature during experiment period; DCT = drying chamber temperature; AT = atmospheric temperature.

In addition, heat generation in the air inlet section, exit section, and ambient air were measured during the drying of potatoes and bananas to estimate the dryer efficiency. Data are depicted in Table 3. The efficiency was calculated using Equation (1). Table 3 shows that average inlet, outlet, and ambient temperatures are 62.5 °C, 55.4 °C, and 40.8 °C, respectively, while dryer efficiency is found to be 32.3%.

Table 3. Dryer efficiency.

Section	Average Temperature (°C)	Dryer Efficiency (%)
Air inlet	62.5	
Air exit	55.4	49.2
Ambient	40.8	

3.2. Drying Kinetics

The influence of solar drying and direct sun drying on the drying time of potato slices dried at various dry bulb temperatures was observed. The moisture ratio (MR) versus drying time (hours) is plotted in Figure 5.

Figure 6 presents the drying rate as a function of time and drying method for potatoes. From Figures 5 and 6, one can see that the drying rate was significantly higher in the case of solar drying than direct sun drying. The increased slope indicates more rapid drying. Solar drying took approximately 6 h to achieve equilibrium moisture content. On the contrary, direct sun drying took approximately 9 h to accomplish that moisture content. The drying rate changed with time and increased and decreased with changes in temperature, drying phase, and case hardening (the hardening of the outer surface of the product).

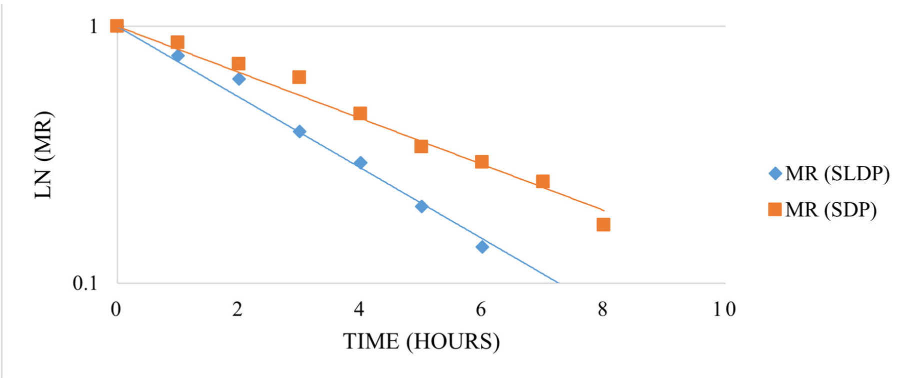

Figure 5. Influence of drying methods on potato slices; SLDP = solar-dried potato; SDP = direct sun-dried potato.

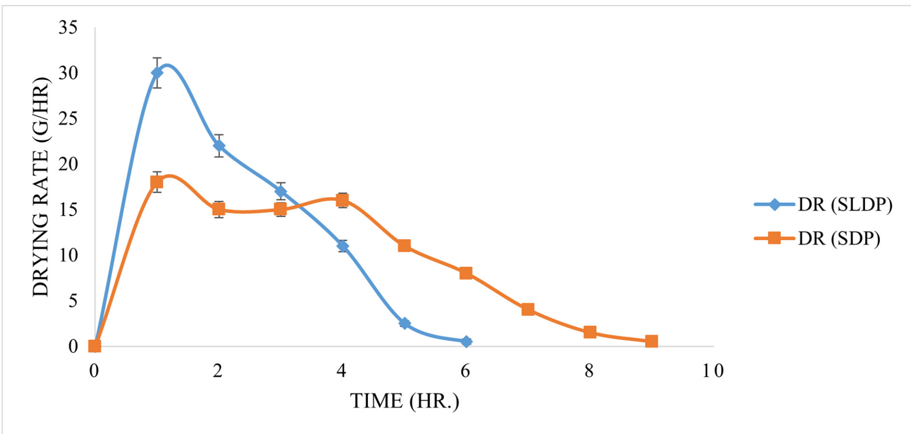

Figure 6. Influence of drying methods on drying rate; SLDP = solar-dried potato; SDP = direct sun-dried potato.

Similarly, for drying banana slices, the moisture ratio (MR) versus drying time (hours) is plotted in Figure 7. The solar drying curve has a more negative slope than direct sun drying, indicating more rapid drying.

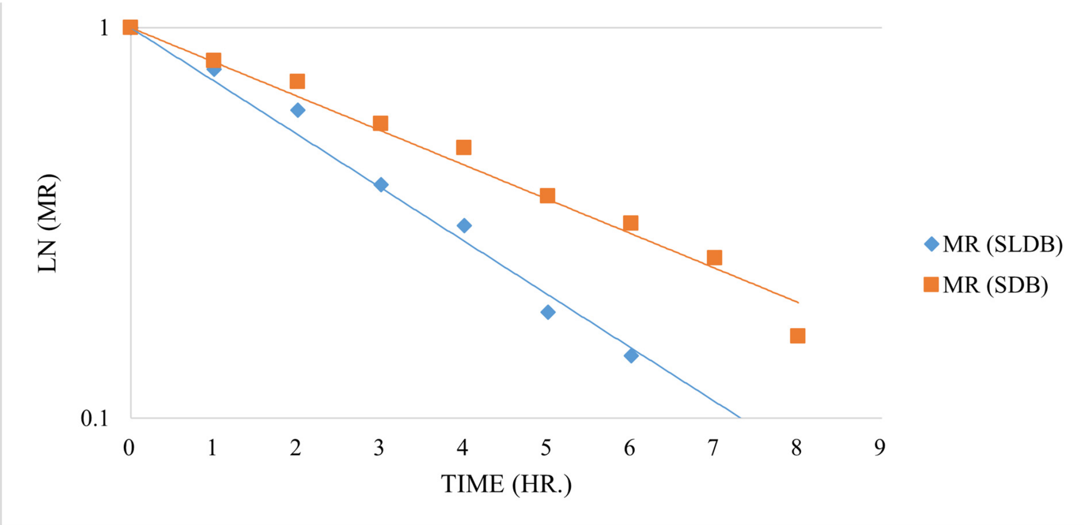

Figure 7. Influence of drying methods on banana slice; SLDP = solar-dried banana; SDP = direct sun-dried banana.

Figure 8 presents the drying rate as a function of time and drying method for bananas. From Figures 7 and 8, it may be concluded that the drying rate was significantly higher in the case of solar drying than direct sun drying. Solar drying took nearly 6 h, while direct sun drying took almost 9 h to achieve equilibrium moisture content.

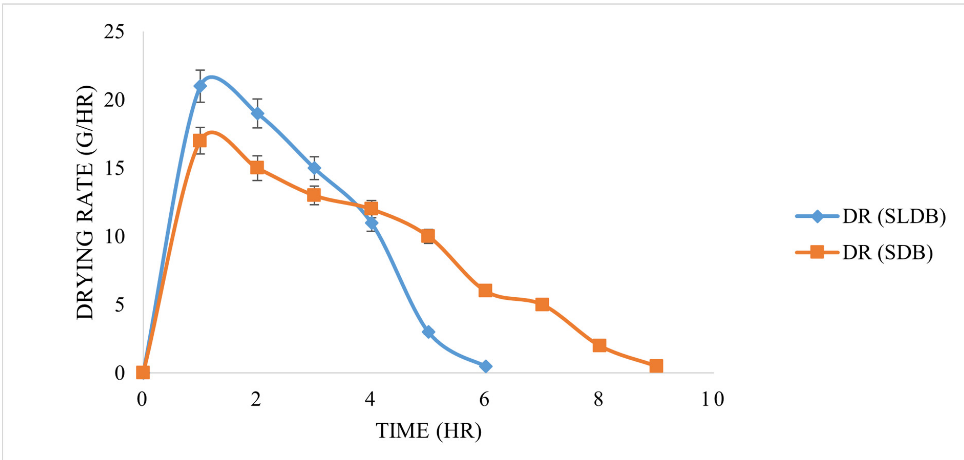

Figure 8. Influence of drying methods on drying rate; SLDP = solar-dried banana; SDP = direct sun-dried banana.

Data for the moisture ratio of potato and banana were analyzed, and regression equations and the Root Mean Square Error (RMSE) were determined and are presented in Table 4. Lower RMSE values indicate better goodness of fit, and, here, a negative correlation was observed for RMSE with drying rate. The sun-dried banana samples showed the lowest drying rate (k = 0.202), while the directly sun-dried potato samples showed the highest rate (k = 0.317). This discrepancy implies that potatoes dry more quickly than bananas when exposed directly to the sun, which is probably caused by differences in their structural makeup, moisture content, and surface area-to-volume ratio. Model accuracy can be inferred using Root Mean Square Error (RMSE) values, where lower

RMSE values indicate a better fit between the drying model and experimental data. The solar-dried potatoes and bananas (RMSE 0.117 and 0.113, respectively) show slightly better fits to their respective models as compared to their direct sun-dried equivalents (RMSE 0.147 and 0.148, respectively).

Table 4. Regression analysis.

Samples	Regression Equation	RMSE
Solar-dried potatoes	$MR = e^{-0.206t}$	0.117
Direct sun-dried potatoes	$MR = e^{-0.317t}$	0.147
Solar-dried bananas	$MR = e^{-0.315t}$	0.113
Direct sun-dried bananas	$MR = e^{-0.202t}$	0.148

3.3. Proximate Composition Analysis

The proximate compositions of dehydrated bananas and potatoes are shown in Table 5. Slices of potatoes and bananas that were sun-dried directly had somewhat lower moisture contents than those that were dried in the solar dryer. Every treated sample included in this investigation had a moisture content of roughly 12–13%, which is appropriate for a longer shelf life [27]. The lower water content found in all tested samples resulted in increased stability and a longer shelf life by reducing the potential for microbial growth and increasing resilience against physical and chemical interactions.

Table 5. Proximate composition analysis. (Data are expressed as mean ± standard deviation; samples with same superscript along each row do not differ at $p \geq 0.05$).

Parameter	Potato		Banana	
	Direct Sun-Dried	Solar-Dried	Direct Sun-Dried	Solar-Dried
Moisture (%)	12.25 ± 1.89	12.14 ± 1.24	12.46 ± 1.16	12.17 ± 1.18
Ash (%)	2.33 ± 0.24	2.31 ± 0.16	2.49 ± 0.16	2.53 ± 0.18
Protein (%)	7.47 ± 0.84	7.23 ± 0.81	3.42 ± 0.66	3.34 ± 0.61
Fat (%)	1.14 ± 0.06	1.19 ± 0.07	1.12 ± 0.06	1.23 ± 0.05
Carbohydrate (%)	76.81 ± 2.14	77.13 ± 2.35	80.51 ± 2.16	80.73 ± 2.16

The difference in ash content between bananas and potatoes was found to be insignificant regardless of the drying method employed. Specifically, the ash content for potato was measured at 2.33% and 2.31%, while for banana, it was 2.49% and 2.53% for direct sun and solar drying, respectively. It is worth noting that the ash content of food represents the total amount of minerals present [28].

Additionally, crude protein content varied depending on the drying method. Direct sun-dried samples exhibited slightly higher protein content as compared to solar-dried samples. This variation is attributable to the intense heat treatment during direct sun drying, which might lead to protein denaturation [29].

Moreover, crude fat content was observed to be higher in solar-dried samples, while direct sun-dried samples exhibited lower crude fat content. This difference can be attributed to the prolonged exposure to air during direct sun drying, which may induce lipid oxidation [30]. Furthermore, the carbohydrate levels of both samples varied in accordance with the moisture, protein, fat, and ash content. Food materials generally contain a significant amount of carbohydrates, reflecting elevated levels of sugars, starches, and dietary fibers [31]. Therefore, both solar- and sun-dried products are good foods.

3.4. Color Analysis

Since fruits and vegetables, which include high amounts of water, carbohydrates, proteins, and lipid components, frequently undergo thermal treatments that change their natural hue, color is an important quality criterion for dried materials [32]. The impact of drying techniques on the color (L*, a*, and b* values) of potatoes and bananas is shown in Table 6.

Table 6. Color analysis. (Data are expressed as mean ± standard deviation; samples with same superscript along each row don't differ at $p \geq 0.05$.)

Parameter	Potato		Banana	
	Direct Sun-Dried	Solar-Dried	Direct Sun-Dried	Solar-Dried
L* (lightness)	57.89 ± 3.24	42.43 ± 3.89	72.17 ± 5.18	63.46 ± 4.16
a* (red/green)	21.12 ± 1.76	17.18 ± 0.74	13.63 ± 1.38	9.49 ± 0.96
b* (yellow/blue)	57.52 ± 4.81	47.78 ± 2.68	43.44 ± 3.61	33.18 ± 3.43

The results revealed a notable contrast in color parameters for each sample under different drying treatments. The L* (lightness) value was lower for bananas dried in the solar dryer, and a similar trend was observed for potatoes. Solar drying led to significant color degradation. Conversely, the a* (red/green) value was moderately lower for bananas as compared to potatoes. In both cases, direct sun-dried samples exhibited relatively higher a* values than solar-dried samples. Similar trends were observed for b* (yellow/blue) values, with solar drying resulting in lower values compared to direct sun drying. The variation in color parameters may be attributable to differences in drying temperature. Lower drying temperatures hinder the Maillard reaction, caramelization, and the degradation of color pigments, thereby preserving the natural color [33]. Consumers desire processed foods to retain their original color. The closer it is to the original color, the more it is acceptable to them. The solar-dryer-dried products were found to be very close to the direct sun-dried products. This is a good indication of color retention of dehydrated products.

3.5. Bioactive Compounds

The phenolic content of the banana and potato samples is displayed in Table 7. The phenolic content of solar-dried samples is somewhat lower than that of direct sun-dried samples. During the drying process, phenolic compounds detach from the oxidative enzyme, leading to structural collapse and breakdown, which liberates more chemicals [33]. When ether and ester covalent bonds break at high temperatures and after prolonged heat exposure, the phenolic is lost [34].

Table 7. Bioactive compounds. (Data are expressed as mean ± standard deviation; samples with same superscript along each row do not differ at $p \geq 0.05$).

Parameter	Potato		Banana	
	Direct Sun-Dried	Solar-Dried	Direct Sun-Dried	Solar-Dried
Phenolic content (mg GAE/100 g)	38.25 ± 1.53 ^{a}	31.25 ± 1.53 ^{b}	63.53 ± 1.23 ^{a}	46.38 ± 1.46 ^{b}
Flavonoid content (mg QE/100 g)	18.60 ± 0.87 ^{a}	14.60 ± 0.87 ^{b}	30.85 ± 0.88 ^{a}	23.94 ± 0.92 ^{b}
DPPH scavenging activity (% inhibition)	36.48 ± 1.17 ^{a}	28.72 ± 1.04 ^{b}	51.87± 1.43 ^{a}	42.28± 1.11 ^{b}

Following exposure to both drying methods, the samples' total flavonoid concentration showed greater values in the case of sun drying. Perhaps because of the greater drying temperature, solar drying decreased the flavonoid concentration of the samples. As flavonoids have functional groups in their nuclear structure, their structure–activity connection also controls their antioxidant ability, scavenging free radicals and chelating action [35]. Because of their advantageous properties, foods containing high levels of phenolics, flavonoids, and antioxidants are regarded as superior quality.

Similar results were observed in terms of antioxidant activity. Direct sun-dried samples exhibited the highest antioxidant activity (percentage inhibition) compared to solar drying. High-temperature drying showed a negative correlation with DPPH scavenging activity, as it denatures polyphenol oxidase and reduces the bioavailability of nutrients and other antioxidant-active substances [36]. High heat treatment reduces the bioactive components of food products, which is an indication of foods with inferior quality.

3.6. Sensory Analysis

Drying procedures significantly impact the modification of sensory characteristics [37,38]. Figure 9 illustrates the average sensory evaluation results as reported by the panel of judges, represented as ratings on a nine-point hedonic scale. Solar-dried potato and banana samples obtained the highest overall acceptance score (8). Conversely, direct sun-dried samples exhibited the best color values. Flavor analysis revealed that banana samples received the highest score (8.0), while solar-dried potatoes scored the highest in terms of texture.

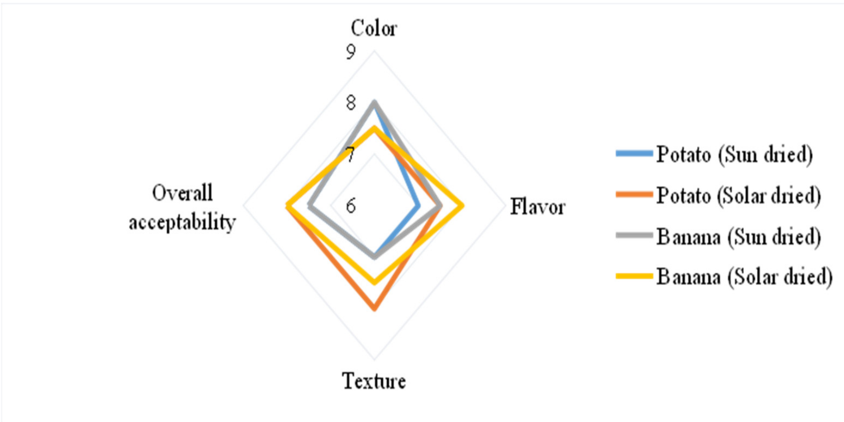

Figure 9. Sensory evaluation.

3.7. Cost Analysis

The cost analysis results are presented in Table 8. The initial cost of the solar dryer and the yearly benefits are the two key factors that determine the payback period. Annual benefit largely depends on the product's selling price. Nine months is considered a suitable drying period for the dryer's use. The value of the economic attribute is 3.26, which is a good indication of profit. Moreover, the values may vary with the climatic conditions as well as market prices. The results agree with the findings of Singh et al. [24] and Poonia et al. [25].

Table 8. Cost analysis.

Parameter	Value
Life Cycle Cost (BDT / USD)	95,176/596.38
Life Cycle Benefit (BDT / USD)	310,651/1946.56
Economic Attribute	3.26
Payback Periods (year)	1

4. Conclusions

The solar dryer functioned quicker as compared to sun drying due to its significantly higher heat generation. The solar dryer was designed to improve efficiency and effectiveness and reduce cost within the context of Bangladesh and other low- and middle-income countries. Providing foamed polyethylene insulation between the mild steel sheet resulted in less heat loss. Thin sheets of perforated stainless steel shelves were used to reduce cost. Solar drying led to slightly lower nutrient retention compared to direct sun drying. Based on the design and performance assessment, the solar dryer outperformed direct sun drying in terms of efficiency and product quality. The findings underscore the potential of this inexpensive solar drying technology to greatly improve agricultural practices and food preservation methods in LMIC as compared to current domestic technology.

Its wider applicability and efficacy may be impacted by operational costs, unmeasured nutritional quality implications, and environmental variability, especially in areas or seasons with less constant sunlight. Future research should address the shortcomings of the current work. These include improving the efficiency of the device by reducing air leakage and increasing solar infiltration to reduce the time to dry the food and thereby increase the device's productivity, by reducing the cost of the solar and electrical components by finding less expensive ones, by supporting manufacturers by training their workers to fabricate the dryer, and by training the users in its proper operation to reduce food losses.

Author Contributions: Conceptualization, A.N.M.A.R., M.S.R. and K.S.I.; data curation, A.N.M.A.R. and M.S.R.; formal analysis, A.N.M.A.R. and M.S.R.; funding acquisition, K.S.I.; investigation, A.N.M.A.R., M.S.R., R.A., M.P.H. and P.K.M.; methodology, A.N.M.A.R., M.S.R. and J.C.; project administration, A.N.M.A.R. and K.S.I.; resources, A.N.M.A.R., M.S.R. and K.S.I.; software, M.S.S.; supervision, A.N.M.A.R. and M.S.R.; validation, M.S.R. and J.C.; visualization, A.N.M.A.R., M.S.R. and K.S.I.; writing—original draft, A.N.M.A.R., M.S.R., R.A., M.P.H. and P.K.M.; writing—review and editing, A.N.M.A.R., M.S.R. and J.C. All authors have read and agreed to the published version of the manuscript.

Funding: The Feed the Future (FtF) Bangladesh Cereal Systems Initiative for South Aisa–Mechanization Extension Activity (CSISA-MEA) of USAID provided funding for this study. The writers' information, assertions, suggestions, ideas, and viewpoints do not necessarily represent those of USAID or the US government.

Data Availability Statement: The raw data supporting the conclusions of this article will be made available by the authors on request.

Acknowledgments: The authors express deep gratitude to CIMMYT and the Georgia Institute of Technology colleagues for their generous and invaluable technical assistance. A special acknowledgment is given to the Department of Agro Product Processing Technology, Jashore University of Science and Technology, for providing laboratory facilities for completing this research.

Conflicts of Interest: The authors declare no conflicts of interest.

References

1. Emad, A.A. Utilization of a solar greenhouse as a solar dryer for drying dates under the climatic conditions of the eastern province of Saudi Arabia. *J. Agric. Sci.* **2012**, *4*, 237–246.
2. Rosegrant, M.W.; Magalhaes, E.; Valmonte-Santos, R.A.; Mason-D'Croz, D. Returns to Investment in Reducing Postharvest Food Losses and Increasing Agricultural Productivity Growth. In *Prioritizing Development: A Cost Benefit Analysis of the United Nations' Sustainable Development Goals*; Lomborg, B., Ed.; Cambridge University Press: Cambridge, UK, 2018; pp. 322–338.
3. Arumugam, S.; Rangarajan, J.M.; Brijesh, K.; Tiwari, A.G. *Brian McKenna, Pulse Foods*, 2nd ed.; Academic Press: Cambridge, MA, USA, 2021; pp. 193–212.
4. Bennamoun, L.; Belhamri, A. Design and simulation of a solar dryer for agriculture products. *J. Food Eng.* **2003**, *59*, 259–266. [CrossRef]
5. Bababola, P.O. Non-convective Solar Pond as a Thermal Energy Source. In Proceedings of the International Conference on Renewable Energy and Climate Change Mitigation, Covenant University, Ota, Nigeria, 13–17 July 2009.
6. Wang, W.; Li, M.; Hassanien, R.; Hassanien, E.; Wang, Y.; Yang, L. Thermal performance of indirect forced convection solar dryer and kinetics analysis of mango. *Appl. Therm. Eng.* **2018**, *134*, 310–321. [CrossRef]
7. Bolaji, B.O.; Olalusi, A.P. Performance evaluation of a mixed-mode solar dryer. *AU J. Technol.* **2008**, *11*, 225–231.
8. Duffie, J.A.; Beckman, W.A. *Solar Engineering of Thermal Processes*, 3rd ed.; Wiley Inter Science: New York, NY, USA, 2006; pp. 9–11.

9. Youcef-Ali, S.; Messaoudi, H.; Desmons, J.Y.; Abene, A.; Le-Ray, M. Determination of the average coefficient of internal moisture transfer during the drying of a thin bed of potato slices. *J. Food Engine* **2001**, *48*, 95–101. [CrossRef]
10. Kalita, P.; Deka, T.J.; Das, S.; Das, D.; Kataki, R. Design, development and performance evaluation of a fluidized bed paddy dryer. *J. Energy Environ. Sustain.* **2018**, *6*, 18–23. [CrossRef]
11. Lamidi, R.O.; Jiang, L.; Pathare, P.B.; Wang, Y.; Roskilly, A.P. Roskilly, Recent advances in sustainable drying of agricultural produce: A review. *Appl. Energy* **2019**, *233–234*, 367–385. [CrossRef]
12. Marinoni, L.; Stellari, A.; Piera Catteneo, T.M. A mild and innovative solar drying process to provide high quality products. *J. Food Meas. Charact.* **2022**, *16*, 662–667. [CrossRef]
13. Akbulut, A.; Durmus, A. Energy and exergy analyses of thin layer drying of mulberry in a forced solar dryer. *Energy* **2010**, *35*, 1754–1763. [CrossRef]
14. Akpinar, E.K. Drying of mint leaves in solar dryer and under open sun: Modeling, performance analyses. *Energy Convers. Manag.* **2010**, *51*, 2407–2418. [CrossRef]
15. Islam, M.N. Use of Solar Energy for Development of Self-Stable Potato Products. Ph.D. Thesis, Royal Veterinary and Agricultural University, Copenhagen, Denmark, 1980.
16. Goyal, R.K.O.M.; Bhargava, V.K. Mathematical modeling of thin layer drying kinetics of apple in tunnel dryer. *Int. J. Food Eng.* **2008**, *4*, 8. [CrossRef]
17. AOAC International. *Official Methods of Analysis of AOAC International*, 22nd ed.; Oxford University Press: New York, NY, USA, 2023.
18. Pearson, D. *The Dictionary of Nutrition and Food Technology*, 5th ed.; Butterworth Publication: London, UK, 1970.
19. Majumder, S.; Das, P.C.; Sami, R.; Ismail, K.; Almushhin, A.; Iqbal, A.; Ranganathan, T.; Mazumder, M.A.R. Effect of spent green tea leaf extracts, butylated hydroxytoluene and repeated freezing-thawing on physicochemical and oxidative properties of Chevon. *J. Biobased Mater. Bioenergy* **2022**, *22*, 56–67. [CrossRef]
20. Chhetry, A.K.; Dhakal, S.; Chaudhary, L.; Karki, K.; Khadka, R.B.; Chaudhary, G.P.; Bastola, T.P.; Poudel, A.; Aryal, P.; Pandey, J. Study of antibacterial activity of root bark, leaves, and pericarp extracts of Diploknema butyracea and evaluation of prospective antioxidant activity. *J. Trop. Med.* **2022**. [CrossRef] [PubMed]
21. Aboshora, W.; Lianfu, Z.; Dahir, M.; Gasmalla, M.A.; Musa, A.; Omer, E.; Thapa, M. Physicochemical, nutritional, and functional properties of the epicarp, flesh, and pitted sample of doum fruit (Hyphaene Thebaica). *J. Food Nutr.* **2016**, *2*, 180–186.
22. Kumar, R.; Patil, M.B.; Patil, S.R.; Paschapur, M.S. Formulation and evaluation of effervescent floating tablet of famotidine. *Int. J. Pharm. Res.* **2009**, *1*, 754–763.
23. Barnwal, P.; Tiwari, G.N. Grape drying by using hybrid photovoltaic–thermal (PV/T) greenhouse dryer: An experimental study. *Sol. Energy* **2008**, *82*, 1131–1144. [CrossRef]
24. Singh, D.; Singh, A.K.; Singh, S.P.; Poonia, S. Economic analysis of parabolic solar concentrator-based distillation unit. *Indian J. Eco. Dev.* **2017**, *13*, 569–575. [CrossRef]
25. Poonia, S.; Singh, A.K.; Santra, P.; Jain, D. Economic Analysis of Inclined Solar Dryer for Drying of Fruit and Vegetables. *Int. J. Agric. Sci.* **2019**, *11*, 9154–9159.
26. Kilanko, O.; Ilori, T.A.; Leramo, R.O.; Babalola, P.O.; Eluwa, S.E.; Onyenma, F.A.; Ameh, N.I.; Onwordi, P.N.; Aworinde, A.K.; Fajobi, M.A. Design and Performance Evaluation of a Solar Dryer. *J. Phys. Conf. Ser.* **2019**, *1378*, 032001. [CrossRef]
27. Nasir, M.; Masood, S.B.; Faqir, M.A.; Kamran, S.; Rashid, M. Effects of moisture on the shelf life of wheat flour. *J. Agric. Biol.* **2003**, *5*, 458–459.
28. Agoreyo, B.O.; Akpiroroh, O.; Orukpe, O.A.; Osaweren, O.R.; Owabor, C.N. The effects of various drying methods on the nutritional composition of Musa paradisiaca, Dioscorea rotundata and Colocasia esculenta. *Asian J. Biochem.* **2011**, *6*, 458–464. [CrossRef]
29. Peizi, S.; Junxin, L.; Xiang, R. Effect of heating on protein denaturation, water state, microstructure, and textural properties of Antarctic krill (*Euphausia superba*) meat. *Res. Sq.* **2022**, *15*, 2313–2326.
30. Cui, K.; Liu, N.; Sun, Y.; Sun, G.; Wang, S.; Yang, M.; Wang, X.; Zhou, D.; Ge, Y.; Wang, D.; et al. Effect of drying processes on the occurrence of lipid oxidation-derived 4-hydroxy-2- hexenal and 4-hydroxy-2-nonenal in Spanish mackerel (*Scomberomorus niphonius*). *Food Sci. Nutr.* **2022**, *11*, 1013–1023. [CrossRef] [PubMed]
31. Abbas, F.M.A.; Saifullah, R.; Azhar, M.E. Differentiation of ripe banana flour using mineral composition and logistic regression model. *Int. Food Res. J.* **2009**, *16*, 83–87.
32. Perera, C.O. Selected Quality Attributes of Dried Foods. *Dry. Technol.* **2005**, *23*, 717–730. [CrossRef]
33. Nesrine, G.R.; Catherine, B.; Nabil, K.; Nourhène, B.M. Effect of air-drying temperature on kinetics of quality attributes of lemon (*Citrus limon* cv. lunari) peels. *Dry. Technol.* **2015**, *33*, 1581–1589.
34. Sulaiman, S.F.; Yusoff, N.A.M.; Eldeen, I.M.; Seow, E.M.; Sajak, A.A.B.; Supriatno, O.K.L. Correlation between total phenolic and mineral contents with antioxidant activity of eight Malaysian bananas (*Musa* sp.). *J. Food Compos. Anal.* **2011**, *24*, 1–10. [CrossRef]
35. Patron, V.; Baas-Dzul, L.; Medina-Torres, N.; Ayora-Talavera, T.; Anchez-Contreras, A.; García-Cruz, U.; Pacheco, N. The effect of drying temperature on the phenolic content and functional behavior of flours obtained from lemon wastes. *Agronomy* **2019**, *9*, 474. [CrossRef]
36. Heim, K.E.; Tagliaferro, A.R.; Bobilya, D.J. Flavonoid antioxidants: Chemistry, metabolism and structure activity relationships. *J. Nutr. Biochem.* **2002**, *13*, 572–584. [CrossRef] [PubMed]

37. Dhakal, B.; Thakur, J.K.; Mahato, R.K.; Rawat, I.; Rabin, D.C.; Chhetri, R.R.; Shah, K.P.; Adhikari, A.; Pandey, J. Formulation of Ebastine Fast-Disintegrating Tablet Using Co-processed Superdisintegrants and Evaluation of Quality Control Parameters. *Sci. World J.* **2022**. [CrossRef] [PubMed]
38. Feguš, U.; Zigon, U.; Petermann, M.; Knez, Z. Effect of drying parameters on physiochemical and sensory properties of fruit powders processed by PGSS-, Vacuum and Spray-drying. *Acta Chim. Slov.* **2015**, *62*, 479–487. [CrossRef] [PubMed]